Analysis of mechanical property and Seismic Behavior of a New Self-Centering Column Base

P.W. Shen[(1)], P. Yang[(2)], X.Y. Tuo[(3)], Y.M. Yang[(4)], J.H. Hong[(5)]

[(1)] *School of Civil Engineering, Chongqing University, China, peiwenshen@cqu.edu.cn*
[(2)] *School of Civil Engineering, Chongqing University, China, Yangpu@cqu.edu.cn*
[(3)] *School of Civil Engineering, University College Dublin, Ireland, xiaoyi.tuo@ucdconnect.ie*
[(4)] *School of Civil Engineering, Chongqing University, China, yangym@cqu.edu.cn*
[(5)] *School of Civil Engineering, Chongqing University, China, hongjihao1993@163.com*

Abstract

Conventional seismic resistant structures, such as steel moment resisting frames, are designed to experience significant inelastic deformations under strong earthquakes. Inelastic deformations result in damage in structural members and residual story drifts, which lead to high repair costs and disruption of the building use or occupation. Earthquake resilient structure is a new branch of the seismic structural design. The new structural system is not only capable of preventing from the structure failure so as to protect people's life safety during an earthquake, but also restoring immediately the structural function after an earthquake. The self-centering column base is one type of earthquake resilient structure. The paper presents a new self-centering RC column base with steel shoes which is typically designed as full strength to ensure that plastic hinges develop in the bottom end of the first-story columns under strong earthquakes. The column base uses post-tensioned high-strength steel bars to control rocking behavior and energy dissipation fuses to dissipate seismic energy. Based on the analysis of mechanical properties, seismic behavior of the column base under different axial compression ratio was simulated and analyzed by finite element method, and compared with the results of low cyclic loading test. The results indicated that load transfer mechanism of self-centering column base agreed well with the theoretical analysis, only energy dissipation fuses appeared plastic deformation, and residual deformation of structure was small after unloading. The self-centering column base in this paper possess characteristic of resilient structure. Numerical simulation that used OpenSEES finite element software was consistent with test in the aspects of hysteretic curve, peak value point at each level and opening situation of column base under different axial compression ratio. The error of numerical simulation and test results was less than 5%, which proved the validity of the finite element model. The area of prestressed bar, initial stress of prestressed bar, area of energy dissipative element, axial compression ratio are important parameters for evaluation of self-centering capability and energy dissipation capability. According to the results of numerical simulation, the yield strength and loading capacity of self-centering column is directly proportional to the parameters mentioned above. The self-centering capability is directly proportional to area of prestressed bar and initial stress of prestressed bar, but it is inversely proportional to area of energy dissipative element, axial compression ratio. The equivalent viscous damping coefficient and ductility coefficient are used to evaluate energy dissipation capability and ductility of structure, respectively. The area of the energy dissipation element has a significant effect on the energy dissipation capability of self-centering column base, meanwhile axial compression ratio affects ductility. The SC parameter which is related to area of prestressed bar, initial stress of prestressed bar, area of energy dissipative element is proposed. The optimized range of SC parameter is confirmed under different axial compression ratio, and it provides reference for design of the self-centering structure.

Keywords: column base; self-centering; axial compression ratio; design parameter; seismic behavior

1. Introduction

The traditional reinforced concrete frame (RC frame) dissipates seismic energy through plastic deformation of the beam-column members during earthquake loading, but it leads to large and irreparable plastic residual deformation of the structure. Especially, when the column base undergoes large deformation, the cost of structural repair will greatly increase or even cannot be repaired, which result in huge economic losses.

To avoid damage and permanent drift in frame, some scholars have proposed the self-centering structure, which can effectively reduce or even eliminate the residual deformation of the structure. Priestley et al. [1] firstly proposed self-centering post-tensioned precast concrete frames, its column and beam are prefabricated components connected by post-tensioned steel bars. The beam ends are brought into contact with and connected to the column, and the seismic energy is dissipated through the opening and closing of the contacted surface during earthquake. Cheok et al. [2] studied this connection under the low cyclic loading test. The failures in the test were: the beam-column contact surface was opened, the pre-stressed steel was yielded, and the concrete of contact surface is crushed. El-Sheikh et al. [3] calculated a 6-story self-centering concrete frame structure by static elastoplastic analysis and elastoplastic time-history analysis. It shows that the self-centering frame has good strength, stiffness, ductility, better self-centering performance and energy dissipation capability under earthquake loading. Guo et al. [4-5] proposed a beam-column connection of self-centering prestressed concrete (SCPC) frame with web friction devices, adding steel jacket at the beam end, pre-embedded steel plates on the column to prevent stress-concentrated concrete crushing at the joints, and specially set friction plates to dissipate seismic energy. Test results show that the SCPC frame has good seismic performance. On this basis, in order to further study the performance of the self-centering joint in the structure, Guo et al. [6] carried out an elastoplastic time-history analysis of 6-story 4-bay SCPC frame with web friction devices, which achieved the expected goals. Cai et al. [7-8] designed a prefabricated self-centering reinforced concrete joint. The beam is connected to the column through prestressed tendon, energy dissipation elements and high-strength bolts, and the joint is subjected to low cyclic test. Subsequently, numerical simulation analysis of the joint was carried out, and the seismic performance was better by comparison with the test. Pan et al. [9] used ABAQUS finite element software to simulate full scale steel frame beam-column joints and analyzed the parameters. It was concluded that self-centering beam-column joints have desirable strength, stiffness and ductility when appropriate parameters are selected, which demonstrate the expected self-centering capability and energy dissipation. Jiang et al. [10] used ANSYS finite element software to simulate self-centering steel frame structure, and established different model by changing the initial stress of prestressed tendons. It is concluded that as the initial prestress increases, the rigidity, bearing capacity and self-centering capability of the steel frame increase, but the energy dissipation capability decreases. Mirzaie et al. [11] proposed a new self-centering steel frame column base joint, focusing the deformation on the T-stubs energy dissipation device, effectively avoiding the plastic hinge of the column base, and using OpenSEES software to accurately predict the characteristic behavior of the self-centering column base which is similar to ordinary self-centering structure under low cyclic loading. Guo et al. [12-14] proposed a self-centering bridge pier. Through low cyclic test and quasi-static analysis and dynamic time-history analysis, it shows that the self-centering pier joint has good self-centering performance and energy dissipation capability and the bearing capacity is better than the traditional pier.

For study on the self-centering concrete frame column base joints, the concrete at the edge of the column base joint is prone to local damage. The current research pays insufficient attention to the performance of the joint under different axial pressure ratios, and there are few studies on the replacement of energy dissipation elements after earthquake. Therefore, this paper is based on a self-centering column base with steel jacket and replaceable energy dissipation elements. The finite element model is established by OpenSEES software, and the simulation results are compared with the low cyclic loading test results to verify the validity of the model. On this basis, for the different initial stress, area of prestressed tendons, energy dissipation elements area and axial compression ratio, the seismic behavior of self-centering column base is mainly studied, mainly, the principle of how self-centering ability and energy dissipation performance are influenced.

2. Configuration and mechanics mechanism of self-centering column base

2.1 Configuration

The self-centering RC frame column base is disconnected from the foundation, and a steel jacket is placed at the bottom of the column to be in contact with the base steel plate. This structure effectively prevents local crushing of the column bottom and the base concrete. A shear connector is placed at the junction of the base and the column to prevent the column from moving laterally under horizontal load. In the middle of the column, a non-bonded prestressed steel strand penetrating through the column body to the base is arranged. When the column is laterally moved, the bottom of the column rotates with the opening of the contact surface, and the tensile force of the steel strand increases, and the tension of the steel strand is used to realize self-centering performance of the column base, as shown in Fig.1.

The energy dissipation fuse (ED fuse) is composed of a steel bar and a buckling-proof outer sleeve, disposed on the bottom of the column, and the two ends are respectively hinged to the top surface of the base and the upper part of the steel jacket. When the bottom of the column rotates, the steel bars on one side are yielded. On the other side, the steel bars are subjected to compression to achieve energy dissipation.

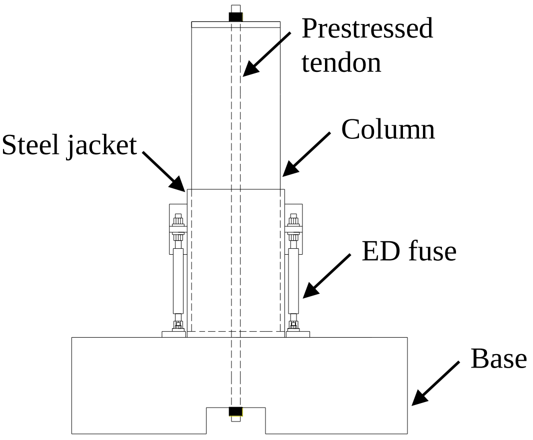

Fig. 1 Self-centering column base configuration

2.2 Mechanics mechanism

The mechanical properties of the self-centering RC frame column base are mainly determined by three parts: prestressed tendon, ED fuse and column. During the whole process, the prestressed tendon is still elastic, and the ED fuse and the column are plastically deformed. The whole working process of column base can be divided into six stages. The typical hysteretic curve is shown in Fig.2.

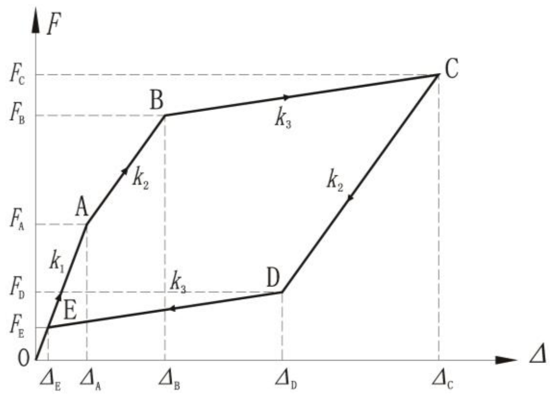

Fig. 2 Typical hysteretic curve

OA stage: At point O, column base is only affected by the axial force. As the horizontal displacement increases, the bending moment of the column increases, and the height of the concrete compression zone at the bottom of the column base gradually increases. When point A is reached, the column and the foundation are in a critical state of contacting. The bending stiffness K_1 of the column at this stage is mainly provided by the concrete column itself.

AB stage: The horizontal displacement continues to increase, and the bottom of the column and the base separate at point A. The lateral stiffness K_2 of the column after separation is provided by the prestressed tendon and the ED fuse. The column body rotates around one side of the column base, prestressed tendon and ED fuse begin to be stretched in the elastic range. When point B is reached, the ED fuse begins to yield.

BC stage: At point B, the ED fuse has yielded. As the horizontal displacement continues to increase to point C, ED fuse is always in a tensile strengthened state, which provides a reduced bending stiffness for the column. At this stage, the prestressed tendon is still in an elastic state, and the bending rigidity provided by the column is constant. Therefore, the bending stiffness K_3 of the column at this stage is mainly provided by the prestressing tendons, which is smaller than the AB stage.

CD stage: Horizontal unloading process, ED fuse and prestressed tendon are in an elastic unloading state. Due to the self-centering action of the prestressed tendon, ED fuse will be unloaded from the tension state of point C until it reaches the point D which subjected to compression and yield. Therefore, the bending stiffness of the column at this stage is the same as that of the AB stage.

DE stage: The ED fuse at point D have been compression yielded and continues to be unloaded to point E, and ED fuse is strengthened due to compression. At point E, the opening between column and base is closed. At this stage, ED fuse and prestressed tendon provide the column with the same bending stiffness as the BC section.

EO stage: At point E, the column and the base are contacted again, and the stress of column is the same with the ordinary RC frame column. The bending stiffness is equal to the OA stage.

3. Simulation analysis

3.1 Finite element model

The test specimen and finite element model (FEM) of the self-centering RC frame column base joint are shown in Fig.3. The height is 1.5 m, and the loading point is 1.3 m from the base, the section dimension is 300 mm×300 mm, the concrete is C60, and the prestressed tendons are two steel strands with a diameter of 15.2 mm, the ultimate strength f_{ptk} is 1860 MPa, the initial stress is controlled to 200 kN (about 0.4 f_{ptk}), and the cross-section area A_{pt} is 280 mm^2.

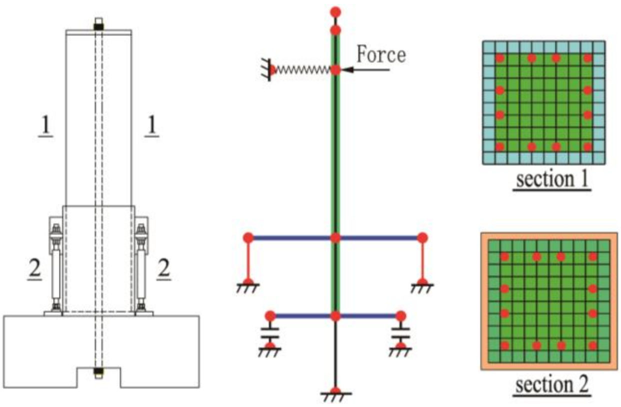

Fig. 3 The finite element model

The two-dimensional FEM is established based on the finite element program OpenSEES. The concrete constitutive model adopts the Concrete01 uniaxial material model, which is based on the Kent-Scott-Park continuous model [15]. The loading and unloading adopt the Karasan-Jirsa criterion. The Hysteresis principle considers the concrete damage by the slope attenuation of the unloading section, and does not consider the tensile performance of the concrete. The steel bars used in column (HRB500) and ED fuse (HPB300) are all modeled with the steel02 uniaxial material, which uses the Giuffre-Menegotto-Pinto model [16]. The unbonded prestressed tendon uses the steel01 uniaxial steel constitutive model, and the initial stress of the prestressed tendon is simulated by the material with initial stress.

The Column which use displacement-based nonlinear element is divided into upper and lower parts. The upper part is reinforced concrete part, the lower part is steel jackets wrapped reinforced concrete part. All parts adopt fiber section. Column section is divided into fibers, and each fiber has a corresponding stress-strain relationship. The upper reinforced concrete part is composed of three different fibers: longitudinal steel bar, confined concrete and unconstrained concrete. The lower reinforced concrete part wrapped with steel jackets is composed of three different fibers: steel plates, longitudinal steel bar and confined concrete. Two fibers cross-section transmits the internal force through the same node [17, 18]. The prestressed tendon uses elastic elements and separate from the column fiber element. The top node of the element shares node with the column and the bottom node is hinged to the base. The ED fuse using HRB300 steel bars adopt the element that only support axial deformation. The compression-free elastic element and the Zero-Length Element are used to simulate the gap between column and base. The rigid arm element whose elastic modulus of the material is magnified 1000 times to ensure that the rigid arm element is not deformed effectively connect ED fuse with column. The rigid arm element transmits the displacement and the in-plane rotation angle of two-dimensional plane in both directions to ensure that the connected objects work and deformation together. The spring element use steel02 uniaxial material and Truss Element to simulate the rolling friction of the column top and the reaction beam. The friction is equivalent to the reaction force generated by setting spring element at horizontal loading point.

3.2 Loading system

Each specimen is exposed gravity loading at first, and then the prestressed tendon is preloaded. Next, a cyclic lateral load is applied to specimens using the displacement-based loading history. The maximum horizontal displacement on the top of the column is 55 mm (story drift is about 0.04 rad). The first loading displacement is 5 mm, and the increment is 5 mm. Every cycle contains a set of positive values and a set of equal negative values. The test setup is shown in Fig.4.

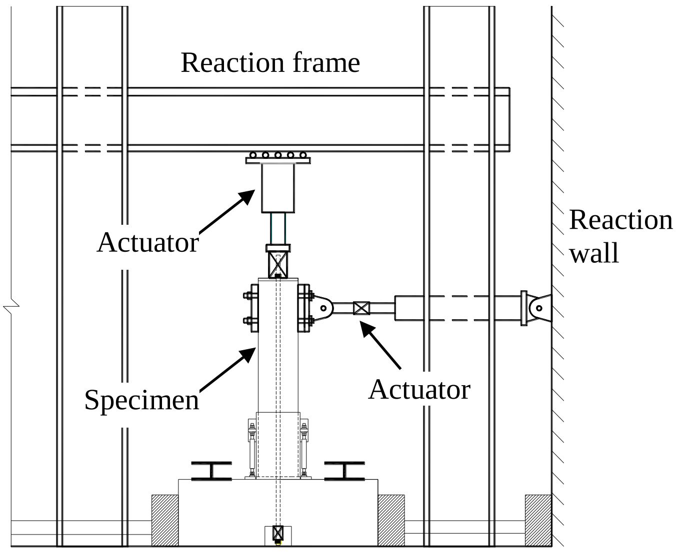

Fig. 4 Test setup

4. Comparative analysis of simulation and test results

4.1 Hysteresis curve

By establishing the OpenSEES FEM, the numerical simulation results are compared with the test load-displacement curves, as shown in Fig.5. The specimen SCFC-0.1 applied 400 kN vertical load (low axial compression), and the specimen SCFC-0.3 applied 1200 kN vertical load (high axial compression).

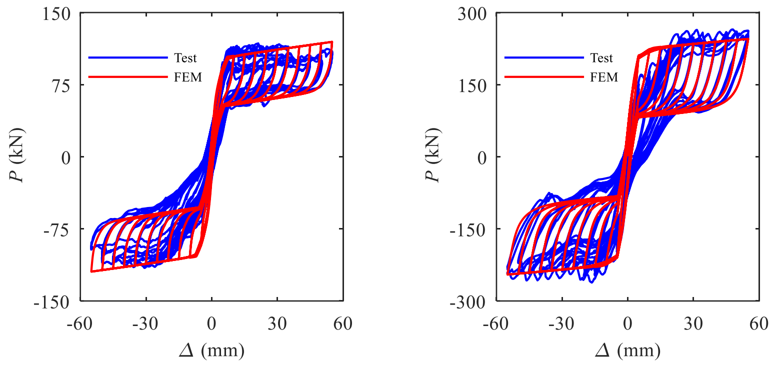

Fig. 5 Hysteresis curves (Left: SCFC-0.1; Right: SCFC-0.3)

The hysteresis curves obtained by simulation and test show the typical 6-stage stress of the self-centering RC frame column base joints. The load-displacement hysteresis curves are in good agreement, showing obvious "flag-shaped" shape, indicating the good validity of the FEM.

For the specimen SCFC-0.1, when the positive horizontal displacement does not exceed 35mm, the hysteresis curve of the simulation and the test are basically the same. When the horizontal displacement exceeds 35mm, the simulated ultimate capacity is obviously larger than the capacity in test. Because in the test, ED fuse on the right side of the column destroy due to the accumulation of damage during multiple cycles of compression and tension, while the ED fuse in FEM does not destroy in the later cycles. When the horizontal displacement is negative, the hysteresis curve of the simulation and the test is quite different. The reason is that the prestressed tendon has a large loss when the column moves sideways and the crack development of the column is relatively sufficient. It causes the significant reduction of lateral stiffness when column is loaded and unloaded, meanwhile, the capacity is significantly reduced under each level of horizontal displacement. In the FEM, the column is intact and the prestressed tendons do not lose capacity. And the simulation curve is also symmetric in loading and unloading. For the specimen SCFC-0.3, when the horizontal displacement is positive, the unloading section of the hysteresis curve of the simulation and the test differs greatly because one of the two nuts sandwiching the upper part of the ED fuse is loose, which cause the nuts to be stressed when column is loaded in the forward direction. At stage of loading, the loose nut causes the ED fuse partially in work. At stage of unloading, the loose nut causes the ED fuse not in work, so that the unloading stiffness is less than the loading stiffness. Moreover, there is a large residual deformation in the test because concrete is cracked between the column and the steel jacket, but the column element remains elastic in the software simulation. When the horizontal displacement is negative, the software simulation results are not much different from the test results in terms of capacity. The simulation and test results of the specimens show that the residual displacement of the specimen SCFC-0.3 is large, indicating the principle that the larger axial compression ratio of the specimen act larger residual displacement and lower self-centering capability.

4.2 Horizontal peak force for each stage

In order to compare the mechanical properties of load-displacement curves by simulation and test, the horizontal peak force under each horizontal control displacement on the hysteresis curve is taken, and summarized in Table 1.

Table 1 Comparison of simulation and test

SCFC-0.1				SCFC-0.3			
Δ	**FEM**	**Test**	**Deviation**	**Δ**	**FEA**	**Test**	**Deviation**
mm	**kN**	**kN**	**%**	**mm**	**kN**	**kN**	**%**
5	82.96	79.66	4.14	5	173.35	165.42	4.80
10	94.30	91.16	3.44	10	200.11	191.09	4.72
15	101.35	98.60	2.79	15	223.98	213.91	4.71
20	108.12	107.91	0.19	20	230.30	223.19	3.19
25	109.80	111.98	-1.95	25	232.63	223.30	4.18
30	111.44	113.59	-1.89	30	234.87	229.20	2.47
35	113.06	111.66	1.25	35	237.01	232.28	2.03
40	114.68	103.33	10.98	40	239.08	234.75	1.85
45	116.28	105.70	10.01	45	241.11	242.29	-0.49
50	117.89	103.05	14.40	50	243.11	234.21	3.80
55	119.50	102.06	17.08	55	245.08	245.41	-0.13

It can be seen from the table that when the horizontal displacement does not exceed 35 mm, the deviation between the simulation value and the test value of the horizontal maximum load of each level is basically within 5%. When the horizontal displacement exceeds 35 mm, the deviation is relatively large, because one of the ED fuses is failure in the test. The deviation of the simulation value and the test value of the horizontal maximum load of each level is basically all within 5%, indicating that the simulation value agrees well with the test value.

4.3 Axial deformation of ED fuse

In order to compare the ED fuse axial deformation in the left and right side of the two specimens during simulation and test, the tensile displacement-loading step curve of the ED fuse is made, as shown in Fig.6.

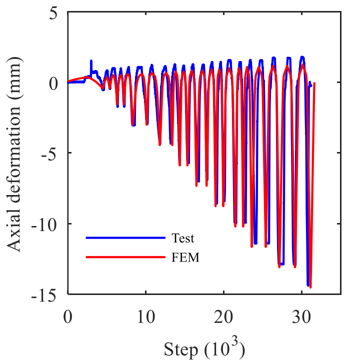

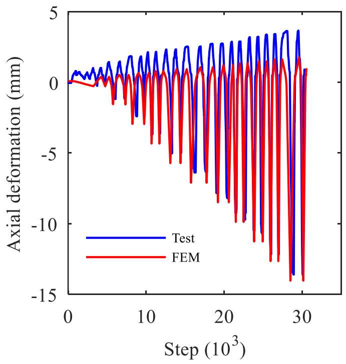

Fig. 6 Displacement-loading step curves of left side ED fuse (Left: SCFC-0.1; Right: SCFC-0.3)

It can be seen from the figure that under the control of horizontal displacement loading in each stage the test results and simulation results are basically the same for the displacement-loading step curve on the left side of SCFC-0.1 and SCFC-0.3. It indicates that the yield energy dissipation of ED fuse on the left and right side approximately the same in the software simulation and test, which verifies the accuracy of the analytical model.

4.4 Prestressed tendon stress

Due to installation and construction error of specimen in the test, the stress of prestressed tendons is asymmetrical. The stress results of prestressed tendons in the software simulation and test are compared to explore mechanical properties, as shown in Fig.7.

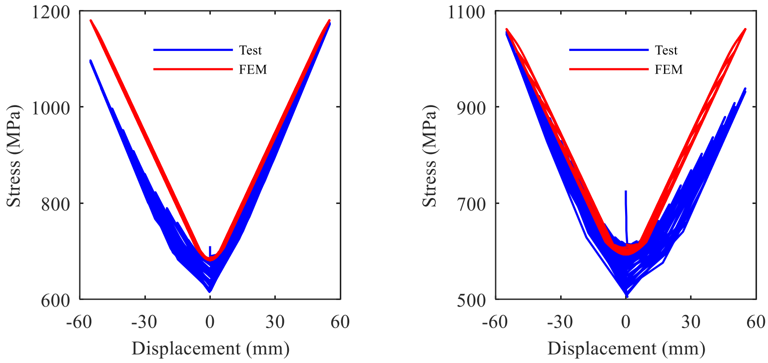

Fig. 7 Prestressed tendon stress (Left: SCFC-0.1; Right: SCFC-0.3)

The stress curve of the prestressed tendons by simulation is basically straight and symmetrical. Compared with the stress curve by the test, it can be seen that the prestressed tendons have obvious loss during the test; the stress values of the prestressed tendons in the test are asymmetric, because there are deviations in the components production. Under the horizontal low cyclic loading test, the vertical load of the column is eccentric, and gap openings on the left and right side of column are not the same, which causes the prestressed tendons in the middle of the column to have different tension degrees.

5. Analysis of seismic behavior by different parameters

According to the test and simulation analysis, the influencing factors include prestressed tendons, ED fuse and axial compression ratio. The seismic performance of the self-centering column base is analyzed.

5.1 Influence of prestressed tendon and ED fuse

The effects of the initial stress (σ_0), the prestressed tendon area (A_{PT}), and ED fuse area (A_{ED}) on the seismic performance of the self-centering column base are studied. The simulation examples are listed in Table 2. The prestressed tendons are 1860 grade, and the ED fuse have a yield strength of 300 MPa.

Table 2 Simulation results I

Number	**SC01**	**SC02**	**SC03**	**SC11**	**SC12**	**SC13**	**SC21**	**SC22**	**SC23**
σ_0/MPa	372	372	372	744	744	744	1116	1116	1116
A_{PT}/mm^2	860	860	860	860	860	860	860	860	860
A_{ED}/mm^2	500	1000	1500	500	1000	1500	500	1000	1500
Number	**SC31**	**SC32**	**SC33**	**SC41**	**SC42**	**SC43**	**SC51**	**SC52**	**SC53**
σ_0/MPa	372	372	372	744	744	744	1116	1116	1116
A_{PT}/mm^2	1720	1720	1720	1720	1720	1720	1720	1720	1720
A_{ED}/mm^2	500	1000	1500	500	1000	1500	500	1000	1500

The load-displacement curves with different parameters are shown in Fig.8. With the area of prestressed tendon, the initial stress of prestressed tendon, and the area of ED fuse increasing, the yield strength and the self-centering capability increase. With the area and initial stress of prestressed tendon increasing, the residual deformation is reduced. With the area of ED fuse increasing, the energy dissipation capability of the self-centering column base is significantly increased, but the residual deformation is also increased, self-centering capability is reduced.

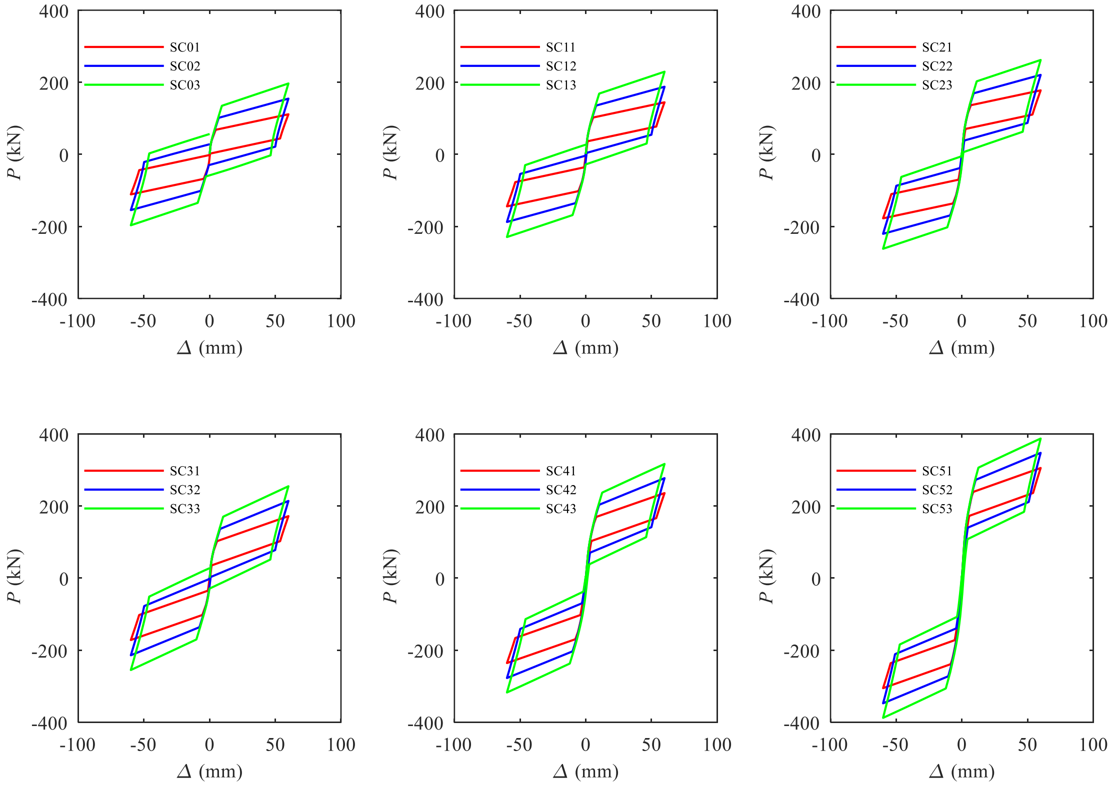

Fig. 8 Load-displacement curves with different parameters

5.2 Axial pressure ratio

The influence of the axial compression ratio on the seismic performance of the self-centering column base are studied. The simulation examples are listed in Table 3. The prestressed tendons are 1860 grade, the initial stress of prestressed tendon is 0.4 f_{ptk}=744 MPa, and the ED fuse have a yield strength of 300 MPa, with area A_{ED}=720 mm^2.

Table 3 Simulation results II

Number	**NF00**	**NF01**	**NF02**	**NF03**	**NF04**	**NF05**	**NF06**	**NF07**	**NF08**
n	0.1	0.15	0.2	0.25	0.3	0.15	0.2	0.25	0.3
A_{PT}/mm^2	860	860	860	860	860	1720	1720	1720	1720

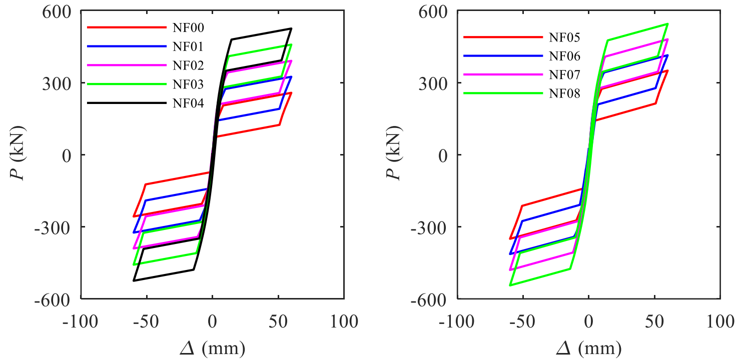

Fig. 9 Load-displacement curves with different axial compression ratio

The load-displacement curves with different axial compression ratios are shown in Fig.9. With the axial compression ratio increasing, the bearing capacity of the self-centering column base increase. Under a larger axial pressure ratio, the bottom of the column base would become nonlinear, and the self-centering capability of the column base reduce, meanwhile, residual deformation increase.

6. Conclusion

By nonlinear analysis through establishing the finite element model of the self-centering RC frame column base joint, the energy dissipation capability and the self-centering capability of RC frame column base joints under different axial compression ratios are compared with the test results. The following conclusions are drawn:

(1) Under different axial compression ratios, the hysteresis curves obtained by simulation analysis and test are in good agreement in the main loading/unloading section, and the self-centering effect is better. For the horizontal load corresponding to the main feature points, the deviation rate between numerical simulation and the test results are within 5%. For the gap opening of the self-centering RC frame column base under the horizontal displacement loading of each level, the difference between simulation and test results is mostly within 5%. The deviation does not exceed 10%, indicating the good validity of the model and results of finite element simulation established in this paper.

(2) Through comparison of prestressed tendons stress, it can be found that the stress is asymmetric in the test due to anchorage deformation and fabrication error, and there is obvious prestress loss, while the simulation cannot consider the influence of the prestress loss. This is where simulation needs to be optimized for improvement.

(3) The yield strength and the self-centering capability of column base increase with the increasement of prestressed tendon area, initial stress of prestressed tendon, ED fuse area, and the axial compression ratio. The self-centering capability increase with the increasement of prestressed tendon area and initial stress. ED fuse area significantly affects the energy dissipation capability of the self-centering column base, and the large axial pressure ratio causes residual deformation increase.

7. Acknowledgements

The research described in this paper was financially supported by the Natural Science Foundation of Chongqing China (cstc2018jcyjAX0061) and the National Natural Science Foundation of China (51578093). Any options, findings, conclusions, or recommendations expressed in this publication are those of the authors and do not necessarily reflect the views of the sponsors.

8. References

[1] Priestley MJN, Tao JR (1993): Seismic response of precast prestressed concrete frames with partially debonded tendons. *PCI Journal*, 38 (1), 58-69.

[2] Cheok GS, Lew HS (1993): Model precast concrete beam-to-column connections subject to cyclic loading. *PCI Journal*, 38 (4), 80-92.

[3] El-Sheikh MT, Sause R, Pessiki S, Lu LW (1999): Seismic behavior and design of unbonded post-tensioned precast concrete frames. *PCI Journal*, 44 (3), 54-71.

[4] Guo T, Song LL, Zhang GD, Gu Y (2012): Experimental study on beam-column connections of self-centering prestressed concrete frame with web friction devices. *China Civil Engineering Journal*, 45 (6), 23-32. [in Chinese].

[5] Guo T, Song LL (2012): Theoretical analysis of beam-column connections of self-centering prestressed concrete frame with web friction device. *China Civil Engineering Journal*, 45 (7), 73-79. [in Chinese].

[6] Guo T, Song LL (2014): Performance-based seismic design method of self-centering prestressed concrete frames with web friction devices. *Journal of Building Structures*, 35 (2), 22-28. [in Chinese].

[7] Cai XN, Meng SP, Sun WW (2012): Experimental study on behaviors of beam-column connections for self-centering post-tensioned precast frame. *China Civil Engineering Journal*, 45 (12), 29-37. [in Chinese].

[8] Cai XN, Meng SP (2016): Numerical analysis for seismic behavior of self-centering post-tensioned precast beam-to-column connections. *Engineering Mechanics*, 33 (3), 143-151. [in Chinese].

[9] Pan ZH, Pan P, Ye LP, Qiu FW (2011): Modeling and parametric study of beam-to-column connection for self-centering steel moment frames. *Journal of Building Structures*, 32 (3), 35-42. [in Chinese].

[10] Jiang CL (2013): Research on seismic behavior of self-centering frame with dissipative elements in the beam-column joints. *Master Dissertation of Suzhou University of Science and Technology*, Suzhou, China. [in Chinese].

[11] Mirzaie M, Bahaari MR, Emam SH (2014): Numerical simulation of the new post tensioned column base with bolted T-stubs. *ISIJ international*, 54 (1), 179-187.

[12] Guo J (2012): Performance based research on the seismic theory and test of new self-centering pier. *Master Dissertation of Tsinghua University*, Beijing, China. [in Chinese].

[13] He MH, Xin KG, Guo J (2012): Local stability study of new bridge piers with self-centering joints. *Engineering Mechanics*, 29 (4), 122-127. [in Chinese].

[14] He MH, Xin KG, Guo J, Guo YJ (2012): Research on the intrinsic lateral stiffness and hysteretic mechanics of self-centering pier. *China Railway Science*, 33 (5), 22-27. [in Chinese].

[15] Scott BD, Park R, Priestley MJN (1982): Stress-strain behavior of confined concrete columns. *ACI Journal*, 79 (1), 13-27.

[16] Menegotto M, Pinto PE (1973): Method of analysis for cyclically loaded reinforced concrete plane frames including changes in geometry and non-elastic behavior of elements under combined normal force and bending. *Proceedings of the IABSE Symposium on Resistance and Ultimate Deformability of Structures*, Lisbon, Portugal.

[17] Qi H, Sun JJ, Lin L (2007): Research on fiber model of OpenSEES. *World Earthquake Engineering*, 23 (4), 48-54. [in Chinese].

[18] Mazzoni S, McKenna F, Scott MH, Fenves GL (2006): The Open System for Earthquake Engineering Simulation (OpenSEES) User Command-Language Manual.

